How to cite:
doi.org/10.1002/anie.202218148

Glycan Editing

Protein-Targeted Glycan Editing on Living Cells Disrupts KRAS Signaling

Yiran Li, Fan Huo, Liusheng Chen, Haiqi Wang, Jianzhuang Wu, Peiwen Zhang, Nan Feng, Wei Li, Lan Wang, Yichun Wang, Xiaojian Wang, Xiaoliang Yang, Zhiqiang Lu, Yang Mao, Chao Yan, Lin Ding,* and Huangxian Ju*

Abstract: The frequent mutation of *KRAS* oncogene in some of the most lethal human cancers has spurred incredible efforts to develop KRAS inhibitors, yet only one covalent inhibitor for the $KRAS^{G12C}$ mutant has been approved to date. New venues to interfere with KRAS signaling are desperately needed. Here, we report a "localized oxidation-coupling" strategy to achieve protein-specific glycan editing on living cells for disrupting KRAS signaling. This glycan remodeling method exhibits excellent protein and sugar specificity and is applicable to different donor sugars and cell types. Attachment of mannotriose to the terminal galactose/*N*-acetyl-D-galactosamine epitopes of integrin $\alpha_v\beta_3$, a membrane receptor upstream of KRAS, blocks its binding to galectin-3, suppresses the activation of KRAS and downstream effectors, and mitigates KRAS-driven malignant phenotypes. Our work represents the first successful attempt to interfere with KRAS activity by manipulating membrane receptor glycosylation.

Introduction

RAS family proto-oncogenes, including the *KRAS* (86%), *NRAS* (11%), and *HRAS* (3%) isoforms, are the most frequently mutated genes in human cancers.[1] RAS proteins respond to upstream stimuli such as growth factor receptors[1,2] and integrins,[3,4] and activate several downstream effector pathways, such as the mitogen-activated protein kinase (MAPK) pathway and the phosphatidylinositol 3-kinase (PI3K) pathway.[1,2] Because of the central role of RAS in driving these signaling networks and malignant phenotypes of cancers including poor prognosis, chemoresistance, and metastasis,[1,2] intense efforts have been undertaken to develop direct and indirect inhibitors for RAS for more than three decades.[1,2] Yet the recent FDA approval of AMG 510,[5] a covalent inhibitor of KRAS-G12 C, has just removed RAS from the list of "undruggable" targets. However, AMG 510 works by covalent adduction to the cysteine residue in $KRAS^{G12C}$ mutants and is therefore only effective in a small fraction of non-small-cell lung cancer patients.[2] Targeting other alleles of *KRAS* mutations is still considered "mission impossible". For the indirect targeting of KRAS signaling, inhibitors of either upstream tyrosine kinase receptors (e.g. epidermal growth factor receptor (EGFR) family) or downstream effectors (e.g. RAF/MEK/ERK/PI3K/AKT) have been developed and some are already in clinical use.[1,2] However, *KRAS* mutations can confer resistance to EGFR inhibitors,[2,3] and the inhibition of one effector pathway is often compensated by the upregulation of other effectors.[1]

Novel and unconventional strategies to target KRAS have also been explored. For example, exosome-delivered siRNA specific to *Kras* was shown to be effective in animal models of pancreatic cancer.[6] Peptides disrupting the interaction between KRAS and its effectors have also been

[*] Y. Li, L. Chen, H. Wang, P. Zhang, N. Feng, W. Li, L. Wang, Y. Wang, Prof. Dr. L. Ding, Prof. Dr. H. Ju
State Key Laboratory of Analytical Chemistry for Life Science, School of Chemistry and Chemical Engineering, Nanjing University
210023 Nanjing (P. R. China)
E-mail: dinglin@nju.edu.cn

F. Huo, J. Wu, Prof. Dr. C. Yan
State Key Laboratory of Pharmaceutical Biotechnology, School of Life Sciences, Nanjing University
210023 Nanjing (P. R. China)
E-mail: yanchao@nju.edu.cn

Prof. Dr. C. Yan, Prof. Dr. L. Ding
Chemistry and Biomedicine Innovation Center (ChemBIC), Nanjing University
210023 Nanjing (P. R. China)

Prof. Dr. X. Wang
Institute of Advanced Synthesis, School of Chemistry and Molecular Engineering, Nanjing Tech University
211816 Nanjing (P. R. China)

Prof. Dr. X. Yang
State Key Laboratory of Coordination Chemistry and Jiangsu Key Laboratory of Advanced Organic Materials, School of Chemistry and Chemical Engineering, Nanjing University
210023 Nanjing (P. R. China)

Prof. Dr. Z. Lu
College of Chemistry and Chemical Engineering and Henan Key Laboratory of Function-Oriented Porous Materials, Luo-yang Normal University
471934 Luoyang (P. R. China)

Prof. Dr. Y. Mao
School of Pharmaceutical Sciences, Sun Yat-sen University
510006 Guangzhou (P. R. China)

developed.[7] A recent work by David Cheresh and colleagues reported the blockage of KRAS-driven oncogenic phenotypes by using polysaccharide GCS-100 to inhibit galectin 3 (Gal-3)–integrin $\alpha_v\beta_3$ interaction.[4] This study gives rise to the interesting question of whether we can regulate KRAS signaling by manipulating the glycosylation state of its upstream membrane receptors, as represented by integrin $\alpha_v\beta_3$. However, the lack of glycan editing tools for the precise tailoring of protein-specific glycan chain structures on living cells has prohibited the answer to this challenging question.

Most membrane receptor proteins are modified by complex glycan chains composed of more than ten types of monosaccharides with varying compositions, sequences, and linkages.[8] The heterogeneity of glycoforms has made both the analysis and manipulation of glycans a daunting task. In recent years, a growing interest in glycobiology has promoted the development of several chemical biology methods to label and edit cell surface glycans, including direct chemical modification,[9] metabolic oligosaccharide engineering (MOE),[10] and chemoenzymatic glycan modification.[11,12] A pioneering work has combined aptamer (Apt) and MOE to label glycans on a specific protein,[10] yet, the Apt recognition-enhanced proximity click reaction leaves a DNA tethered to the metabolically labeled glycans. More recently, a powerful chemoenzyme-based tool has been developed with *N*-glycan-subtype editing selectivity.[12] As to protein-specific glycan editing, a few glycan trimming systems, such as nanobody-fused split *O*-GlcNAcase,[13] antibody–sialidase conjugates,[14] have shown promising prospects in clinical therapy. Despite these remarkable successes, methods enabling the installation of carbohydrates on glycan chains of target proteins remain scarce.

To meet this challenge, herein we sought to develop a protein-specific glycan editing strategy on living cells to precisely tailor glycoforms on membrane proteins, and to explore the possibility of utilizing such a strategy to disrupt KRAS signaling. An ideal glycan editing method should meet the following criteria: 1) confinement on the protein of interest (POI); 2) independence of intracellular processes;[11] and 3) no restrictions on donor sugar structure.

With these in mind, we devised a "localized oxidation-coupling" strategy to install a well-defined carbohydrate on the glycan chains of POI on living cells by orchestrating localized and activatable enzymatic glycan oxidation[15,16] and bioorthogonal aldehyde-hydrazide coupling reaction (Scheme 1A).[17] We designed a glycan remodeling probe that comprises a glycan remodeling module—galactose oxidase (GAO) and a target recognition module—an integrin $\alpha_v\beta_3$-specific peptide ligand c(RGDfK) (Figure S1).[18] GAO can specifically and efficiently oxidize terminal galactose/*N*-acetyl-D-galactosamine (Gal/GalNAc), to generate a bioorthogonal aldehyde group.[19] This group can act as an anchor point to couple hydrazide-modified carbohydrates under physiological conditions to achieve glycan editing.[17] $\alpha_v\beta_3$ is an *N*-glycosylated protein,[20] and the existence of terminal Gal/GalNAc on $\alpha_v\beta_3$ has been observed by several glycoproteomic studies.[21,22] The achievement of protein specificity for GAO oxidation depends on the spatiotemporal control of GAO activity.[15,16] For spatial control, c(RGDfK) directs the probe to $\alpha_v\beta_3$; for temporal control, GAO is inactivated by Fe^{II} ($K_4[Fe(CN)_6]$) during the probe anchoring step to avoid oxidation of non-targeted proteins, and then activated by Fe^{III} ($K_3[Fe(CN)_6]$) to initiate Gal/GalNAc oxidation on $\alpha_v\beta_3$.[15] Using mannotriose (Man_3) as the donor sugar, we demonstrated that this oligosaccharide can be specifically linked to the Gal/GalNAc epitopes of the target protein integrin $\alpha_v\beta_3$ on the surface of living cells and this modification can block the interaction between $\alpha_v\beta_3$ with extracellular Gal-3 (Scheme 1B). The blockade alleviates the activation of KRAS and its downstream effectors and suppresses the malignant phenotypes of KRAS activation in tumor cells. Thus, our novel protein-targeted glycan editing strategy may provide a facile avenue to precisely manipulate the glycoforms of membrane receptor proteins, and the associated recognition behavior and biological functions. Our strategy also holds therapeutic potential for disrupting KRAS signaling through glycosylation intervention.

Results and Discussion

Synthesis of the Glycan Remodeling Probe

We conjugated c(RGDfK)-SH with GAO to prepare the glycan remodeling probe (c(RGDfK)-GAO) (Figure 1A). The successful synthesis of the probe was evidenced by MALDI-TOF MS (Figure 1B) and SDS–PAGE (Figure 1C). The mass spectra of PEG-GAO generated by linking GAO to NHS-PEG1000-MAL showed a significant MS peak shift from m/z 68186 to m/z 70129, indicating the attachment of $\approx$2 PEGs per GAO. The peaks with maximum intensity at m/z 72030 of c(RGDfK)-GAO indicated a product mixture with 1–3 Pep per GAO. The conjugation was further supported by SDS–PAGE image, showing step-by-step up-shifted and smeared bands respectively for PEG-GAO and c(RGDfK)-GAO. Using the $\alpha_v\beta_3$-positive cell line MDA-MB-231 (as manifested in Figure S2), we demonstrated that the probe binding was dependent on c(RGDfK): cyanine 5 (Cy5)-labeled c(RGDfK)-GAO (c(RGDfK)-GAO-Cy5) could bind to MDA-MB-231 cells, whereas two control probes, GAO-Cy5 and PEG-GAO-Cy5, could not (Figure 1D). This binding was substantially inhibited in the presence of excess FITC-labeled c(RGDfK) (Figure 1E).

Protein-Targeted Glycan Remodeling and Labeling

We devised a localized glycan remodeling (LGR) operation, which is opposed to global glycan remodeling (GGR, i.e., using free-diffused GAO to oxidize global Gal/GalNAc on the cell surface). The LGR procedure is carried out as follows: 1) incubating cells with Fe^{II}-inhibited c(RGDfK)-GAO for 30 min followed by removal of unbound probes; 2) activating GAO with Fe^{III} for 30 min. Then, the yielded aldehyde groups on Gal/GalNAc epitopes of POI can be fluorescently labeled with fluorescein-5-thiosemicarbazide

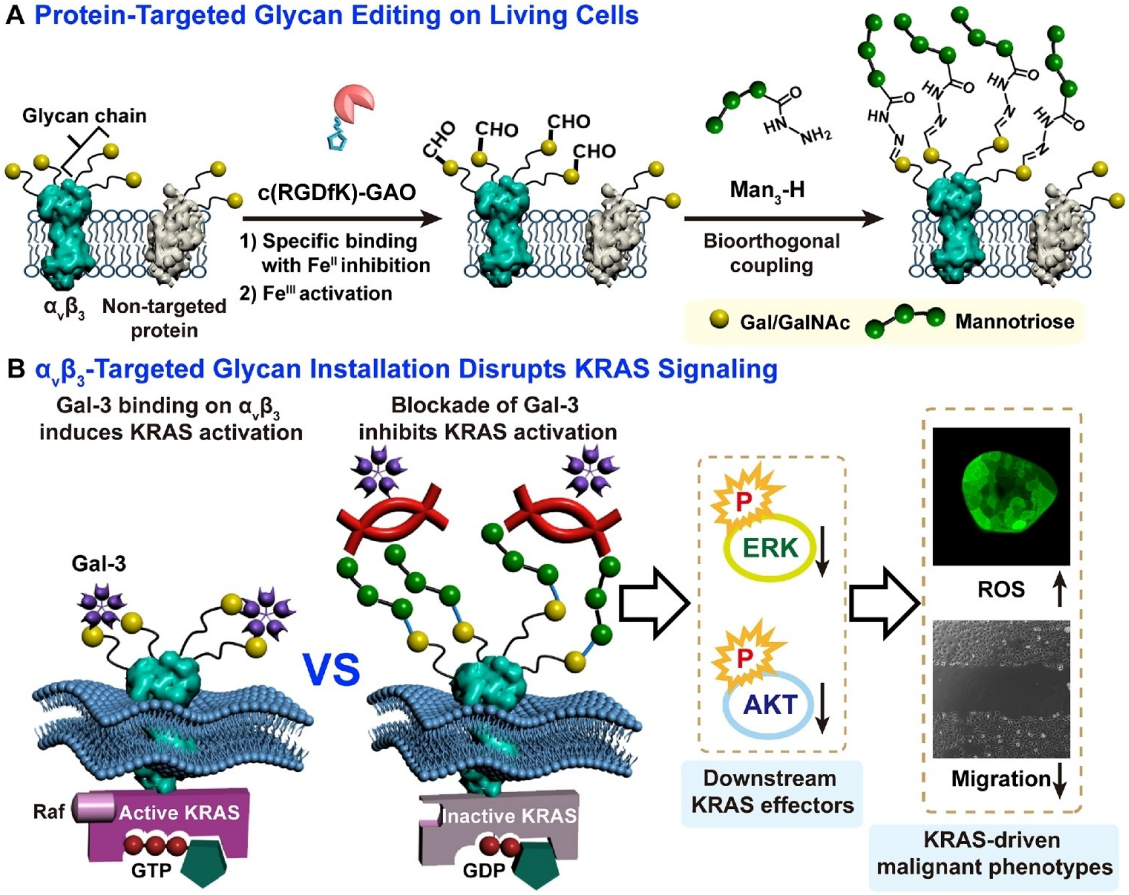

Scheme 1. Schematic illustration of protein-targeted glycan editing on living cells for disruption of KRAS signaling. A) Scheme showing the "localized oxidation-coupling" strategy for the installation of mannotriose (Man_3) on Gal/GalNAc of integrin $\alpha_v\beta_3$. The glycan remodeling probe (c(RGDfK)-GAO) in a Fe^{II}-inactivated state can bind specifically to $\alpha_v\beta_3$ via cyclic peptide-mediated recognition. Then Fe^{III} is added to activate GAO to oxidize the terminal Gal/GalNAc of $\alpha_v\beta_3$-bound glycans to yield aldehyde groups, which can couple to hydrazide-modified Man_3 (Man_3-H) to achieve glycan installation in a protein-specific way. B) The glycan installation blocks extracellular gal-3 binding, alleviates the activation of KRAS and its downstream effectors, and suppresses KRAS-driven malignant phenotypes, including reactive oxygen species (ROS) detoxification and cell migration.

(FTZ) (referred to LGR-F hereafter),[23] affording a facile visualization method for glycans of $\alpha_v\beta_3$ on living cells (Figure 2A, left).

Using living MDA-MB-231 cells as a model, as expected, the fluorescence signal was only observed on the cell surface after Fe^{III} was added (Figure 2B), which represented the Gal/GalNAc level on $\alpha_v\beta_3$. To maximize the fluorescence signal, the incubation time and concentration for the probe were optimized, and 30 min (Figure S3) and 1.5 μM (Figure S4) were chosen, respectively.

We also estimated the LGR labeling efficiency by labeling MDA-MB-231 cells with biotin-hydrazide after LGR (referred to as LGR- B hereafter; Figure 2A, right). western blotting of biotinylated and total α_v and β_3 showed a biotin conjugation ratio of 76 % and 68 % for α_v and β_3, respectively (Figure S5). By combining neuraminidase (Neu)-based sialic acid (Sia) cleavage, the Sia capping ratio of $\alpha_v\beta_3$ was assessed: as low as 24 % in MDA-MB-231 cells (Figure S6).

Demonstration of the Protein and Glycan Specificity of LGR

Next, we verified that the observed fluorescence signal indeed came from Gal/GalNAc of $\alpha_v\beta_3$. We labeled MDA-MB-231 cells with biotin-hydrazide after LGR (LGR-B) or GGR (GGR-B). western blotting (WB) of the corresponding cell lysates with anti-biotin antibody yielded two distinct bands of α_v and β_3 for LGR-B treated cells, but smeared bands for GGR-B treated cells (Figure 2C), demonstrating the $\alpha_v\beta_3$-specificity of LGR. This was further verified by the markedly reduced fluorescence signal on β_3-knockdown cells after LGR-F labeling (Figures 2D, E, S7–S9).

To verify the Gal/GalNAc specificity of our method, we performed three sets of experiments (Figures 2F, G, S10): 1) Adding free Gal during the GAO activation step significantly inhibited the FTZ fluorescence signal on the cell surface. 2) Pretreating cells with tunicamycin (TM), an *N*-glycosylation inhibitor,[24] decreased the FTZ signal to the background level. This is consistent with the fact that $\alpha_v\beta_3$ is an *N*-glycosylated protein.[20,21] 3) In contrast, pretreatment of cells with benzyl-*N*-acetyl-α-galactosaminide (BAG), an

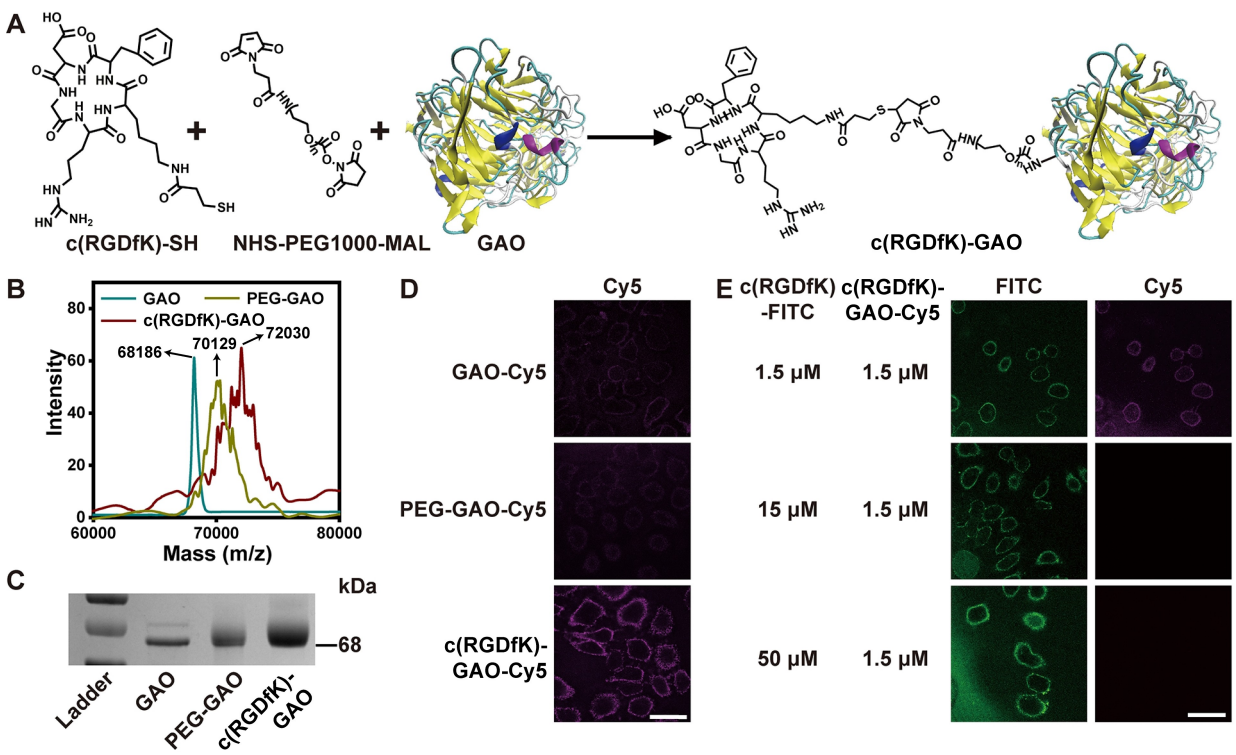

Figure 1. Preparation and characterization of c(RGDfK)-GAO. A) Scheme for the synthesis of c(RGDfK)-GAO. B) Representative MALDI-TOF MS spectra of GAO (cyan), PEG-GAO (mustard), and c(RGDfK)-GAO (wine) from three independent measurements. C) SDS–PAGE image of GAO, PEG-GAO, and c(RGDfK)-GAO. D) Confocal laser scanning microscopy (CLSM) images of cells after incubation with GAO-Cy5, PEG-GAO-Cy5, or c(RGDfK)-GAO-Cy5. E) CLSM images of cells after incubation with a mixture of c(RGDfK)-FITC (of different concentrations) and c(RGDfK)-GAO-Cy5 (1.5 μM). Scale bars: 50 μm. The images are representative of two independent experiments.

O-glycan extension inhibitor,[25] had negligible influence on the FTZ signal. Together, these results prove that c-(RGDfK)-GAO-based LGR is highly specific for Gal/GalNAc of *N*-glycan chains.

We next implemented LGR-F labeling on four additional cell lines to demonstrate the applicability of the method, including the human pancreatic adenocarcinoma cell line Capan-2, the human lung adenocarcinoma cell line A549, the human breast cancer cell line MCF-7 and the mouse embryonic fibroblast cell line MEF^{WT} (Figures 2 and S11). We found that a significant FTZ signal was only observed on cell lines with $\alpha_v\beta_3$-positive expression (Capan-2, A549, and MEF^{WT}, as verified by immunofluorescence and WB (Figures S2 and S12)), whereas the $\alpha_v\beta_3$-negative cell line MCF-7 showed a minimal FTZ signal (Figure 2B). Because of the high expression of $\alpha_v\beta_3$ on MEF^{WT}, we collected biotinylated proteins from LGR-B treated MEF^{WT} and performed label-free qualitative proteomic analysis (Table S1). The proteins with the highest abundance mainly included the integrin family and their interacting glycoproteins (or proteoglycan). This was probably due to the similar sequences shared among different integrin proteins. The α_v and β_3 labeling efficiency on A549 and Capan-2 cells were also analyzed (Figure S5).

Protein-Targeted Glycan Installation

The proposed LGR strategy offers a convenient method for protein-specific editing of Gal/GalNAc-terminated glycan chains on living cells with no restriction on the composition or structure of the donor carbohydrates, provided that they are modified with hydrazide or aminooxy. To demonstrate this, we chose a hydrolysate of plant glycans, Man_3,[26] as the model donor sugar (Scheme 1A). Notably, Mannose impairs tumor growth,[27] and the acquisition of metastatic phenotype is often accompanied by decreased expression of high-mannose glycans on $\alpha_v\beta_3$.[28] We first synthesized hydrazide-functionalized Man_3 (Man_3-H)[29] and characterized it by ^1H NMR and ^{13}C NMR (Supporting Information).

To ensure effective glycan installation, we confirmed that the aldehyde groups artificially generated by either LGR or GGR can stay on the cell surface for at least 24 h (Figure S13). We then performed GGR on MDA-MB-231 cells followed by incubation with Man_3-H to achieve global glycan installation (referred to as GGR-M hereafter). GGR-M-treated cells exhibited much higher binding with a mannose-specific lectin, *Concanavalin* A (Con A),[30] than untreated cells (Figures 3A and B, S14–S16). Next, we performed $\alpha_v\beta_3$-specific glycan editing with Man_3-H (referred to as LGR-M hereafter) by coupling the LGR operation with Man_3-H ligation. This resulted in an elevated level of Man on $\alpha_v\beta_3$, as evidenced by Con A blotting of

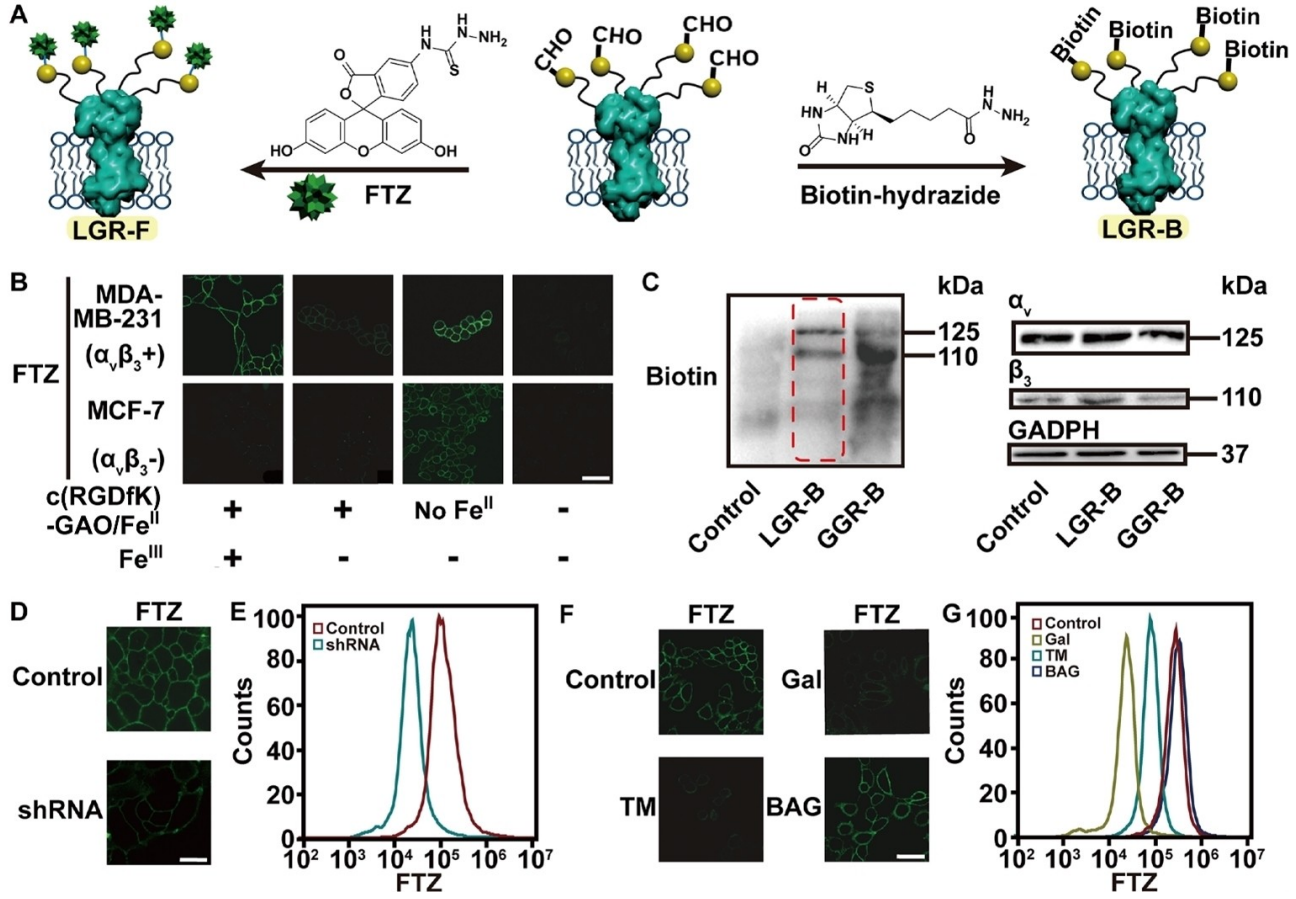

Figure 2. Localized glycan remodeling (LGR) of integrin $\alpha_v\beta_3$ on MDA-MB-231 cells. A) Scheme for fluorescence (LGR-F) or biotin (LGR-B) labeling of $\alpha_v\beta_3$-bound terminal Gal/GalNAc on living cells. B) Demonstration of the successful LGR by CLSM imaging of FTZ fluorescence on $\alpha_v\beta_3$-positive MDA-MB-231 cells (or $\alpha_v\beta_3$-negative MCF-7 cells) after different treatment combinations. C) Demonstration of the LGR protein specificity by WB analysis of lysates of cells undergoing biotin-hydrazide incubation (control), and cells undergoing LGR-B or global glycan remodeling followed by biotin-hydrazide labeling (GGR-B). D), E) Demonstration of LGR protein specificity by knocking down β_3 expression in MDA-MB-231 cells. CLSM images (D) and flow cytometry (FCM) data (E) of $\alpha_v\beta_3$-bound terminal Gal/GalNAc after LGR-F treatment of cells without and with shRNA incubation. CLSM (F) and FCM (G) demonstration of the glycan specificity of LGR by Gal competition or disruption of glycosylation pathways (TM for *N*-glycans, BAG for *O*-glycans). Cells undergoing LGR-F were used as the positive control. Scale bars: 50 μm. All images are representative of three individual experiments, and data are shown as the mean ± SD, $n = 3$.

immunoprecipitated $\alpha_v\beta_3$ from the lysate of LGR-M-treated cells (Figure 3A and B). We also performed MALDI-TOF MS to verify the conjugation of Man_3 to $\alpha_v\beta_3$-carried glycans by LGR-M (Figure S17). The percentage of the oxidized $\alpha_v\beta_3$-carried glycans that were conjugated with Man_3 was quantitatively estimated to be higher than 80 % in all three cell lines tested (Figure S18). We also confirmed, using CCK-8 and Annexin V-FITC/PI apoptosis assays, that glycan editing operations had little effect on cell viability (Figure S19). Taken together, by orchestrating LGR and hydrazide-based sugar ligation, we devised an efficient method for protein-targeted glycan editing.

LGR and Man_3 Installation Blocked the Interaction between $\alpha_v\beta_3$ and Exogenous Gal-3

Next, we tested our method for its ability to intervene in KRAS signaling via the manipulation of the $\alpha_v\beta_3$ glycoform. Previous work by the Cheresh group has demonstrated that integrin β_3, in the presence of Gal-3, can activate KRAS and drive tumor stemness and resistance to EGFR inhibition,[3] which is also related to KRAS addiction.[4] Gal-3, a β-galactoside-binding mammalian lectin,[31,32] can recognize glycan structures like *N*-acetyllactosamine (LacNAc), poly-lactosaminoglycans, GalNAc-α1,3-[Fuc-α1,2]-Gal-β1,4-Glc, NeuNAc-α2,3-Gal-β1,4-Glc, and core 1 (T-antigen), etc. The lectin may cross-link cell surface glycoconjugates to transduce signals due to its multimer structure.

We first investigated the influence of GGR-M and LGR-M treatments on exogenous Gal-3 binding (Figures 3C–E, S20). The $\alpha_v\beta_3$ on MDA-MB-231 cells undergoing LGR-M (or GGR-M) exhibited much lower binding with Gal-3 compared with that on control cells and cells undergoing LGR (or GGR) alone, as reflected by co-immunoprecipitation of $\alpha_v\beta_3$ and Gal-3 (Figure 3C–E). The Man_3-mediated blockade of Gal-3 binding was further evidenced by the decreased co-localization of $\alpha_v\beta_3$ and Gal-3 on cells after

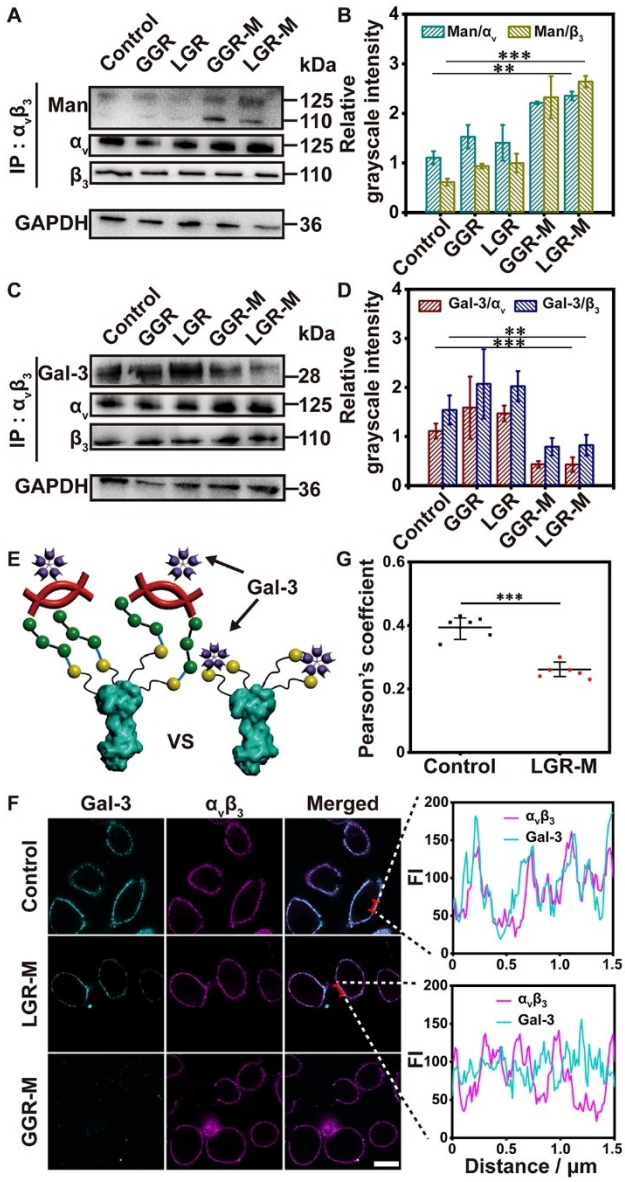

Figure 3. Integrin $\alpha_v\beta_3$-targeted glycan editing on living MDA-MB-231 cells blocks $\alpha_v\beta_3$/Gal-3 binding. A) Con A blotting of immunoprecipitated $\alpha_v\beta_3$ from cells after different treatments. The control group was incubated with Fe^{III} and then Man_3-H. B) Grayscale intensities of Man relative to α_v or β_3 in (A). C) IP-WB demonstration of the blockade effect of Man_3 on the binding between $\alpha_v\beta_3$ and exogenous Gal-3. After different treatments, cells were incubated with Gal-3, and the cell lysates were immunoprecipitated with anti-$\alpha_v\beta_3$ antibody followed by immunoblotting with anti-Gal-3, anti-α_v, or anti-β_3 antibodies. The control is the same as in (A). D) Grayscale intensity analysis of Gal-3 relative to α_v or β_3 in (C). E) Scheme showing the blockade effect of Man_3. F) Immunofluorescence co-localization analysis of Gal-3 (Cyan) and $\alpha_v\beta_3$ (Magenta) in LGR-M or GGR-M treated cells after incubation with Gal-3. Cells only undergoing Gal-3 incubation are the control. The fluorescence plot profiles for both channels of the cell membrane regions marked as red are also shown. G) Co-localization analysis of $\alpha_v\beta_3$ and Gal-3 in (F). Scale bar: 20 μm. The images are representative of three individual experiments, and data are shown as the mean ± SD, $n = 3$. ** $p < 0.005$; *** $p < 0.0005$.

LGR-M treatment (Figures 3F, G and S21). Molecular docking experiments also supported these results: after Man_3 installation, the binding energy of various $\alpha_v\beta_3$-bearing glycans to Gal-3 increased (Table S2).

For comparison, we also synthesized and characterized hydrazide-functionalized *N*-acetyllactosamine (LacNAc-H, Supporting Information), and installed it on $\alpha_v\beta_3$ (referred to as LGR-L). As expected, this resulted in stronger binding of $\alpha_v\beta_3$ with Gal-3 (Figure S22). These data confirm that combining LGR with glycan coupling enables in situ manipulation of glycan recognition behavior on specific receptor proteins.

Disruption of KRAS Signaling via Blocking $\alpha_v\beta_3$/Gal-3 Interaction

Next, we investigated whether blockade of the $\alpha_v\beta_3$/Gal-3 interaction could affect KRAS signaling. We chose the $\alpha_v\beta_3$-positive, $KRAS^{G12V}$ mutant pancreatic cancer cell line Capan-2 (Figure S2) as the representative cell model. Since cellular KRAS protein cycles between a guanosine triphosphate (GTP)-bound active state (KRAS-GTP) and guanosine diphosphate (GDP)-bound inactive state (KRAS-GDP), we utilized glutathione S transferase-tagged RAS-Binding Domain of Raf (GST-Raf-RBD, that specifically binds to KRAS-GTP) to pull down KRAS-GTP in cell lysates (Figure S23)[4] for direct measurement of the KRAS activation level in cells. We also evaluated the activation status of the two major effector signaling pathways downstream of KRAS, RAF/MEK/ERK and PI3K/AKT, by WB. Four groups were included in these experiments and were designated as follows: I) Blank; II) Gal-3; III) LGR-M; and IV) LGR-M→Gal-3 (Figure 4A).

Consistent with previous reports,[33] exogenous Gal-3 alone led to potent activation of KRAS as evidenced by elevated levels of KRAS-GTP, and phosphorylated ERK (pERK) and AKT (pAKT) (Gal-3 vs. Blank). In the presence of Gal-3, LGR-M markedly decreased the levels of KRAS-GTP, pAKT, and pERK (LGR-M→Gal-3 vs. Gal-3), suggesting that LGR-M operation could effectively inhibit Gal-3-elicited, $\alpha_v\beta_3$-mediated activation of KRAS and its downstream signaling. And the inhibition effect was verified to rely on the successful ligation of Man_3 to $\alpha_v\beta_3$ (Figure S24). Thus, we reason that the Man_3 modification of $\alpha_v\beta_3$ glycan chains on Capan-2 cells prevents Gal-3 binding, weakens the clustering of $\alpha_v\beta_3$, which is required for KRAS activation,[3] and diminishes subsequent RAF/MEK/ERK and PI3K/AKT signaling.

To further investigate the applicability of this approach to intervene with KRAS signaling, we extended the above experiments to RAS knockout mice-derived mouse embryonic fibroblast cells (Ras-less MEFs) stably overexpressing the $KRAS^{G12D}$ or $KRAS^{G12V}$ mutation (MEF^{G12D} or MEF^{G12V}). These cells are ideal tools for investigating RAS signaling because of their clean genetic background (https://www.cancer.gov/research/key-initiatives/ras/ras-central/blog/2017/rasless-mefs-drug-screens). In both cell lines, LGR-M significantly inhibited Gal-3-induced KRAS-GTP, pAKT

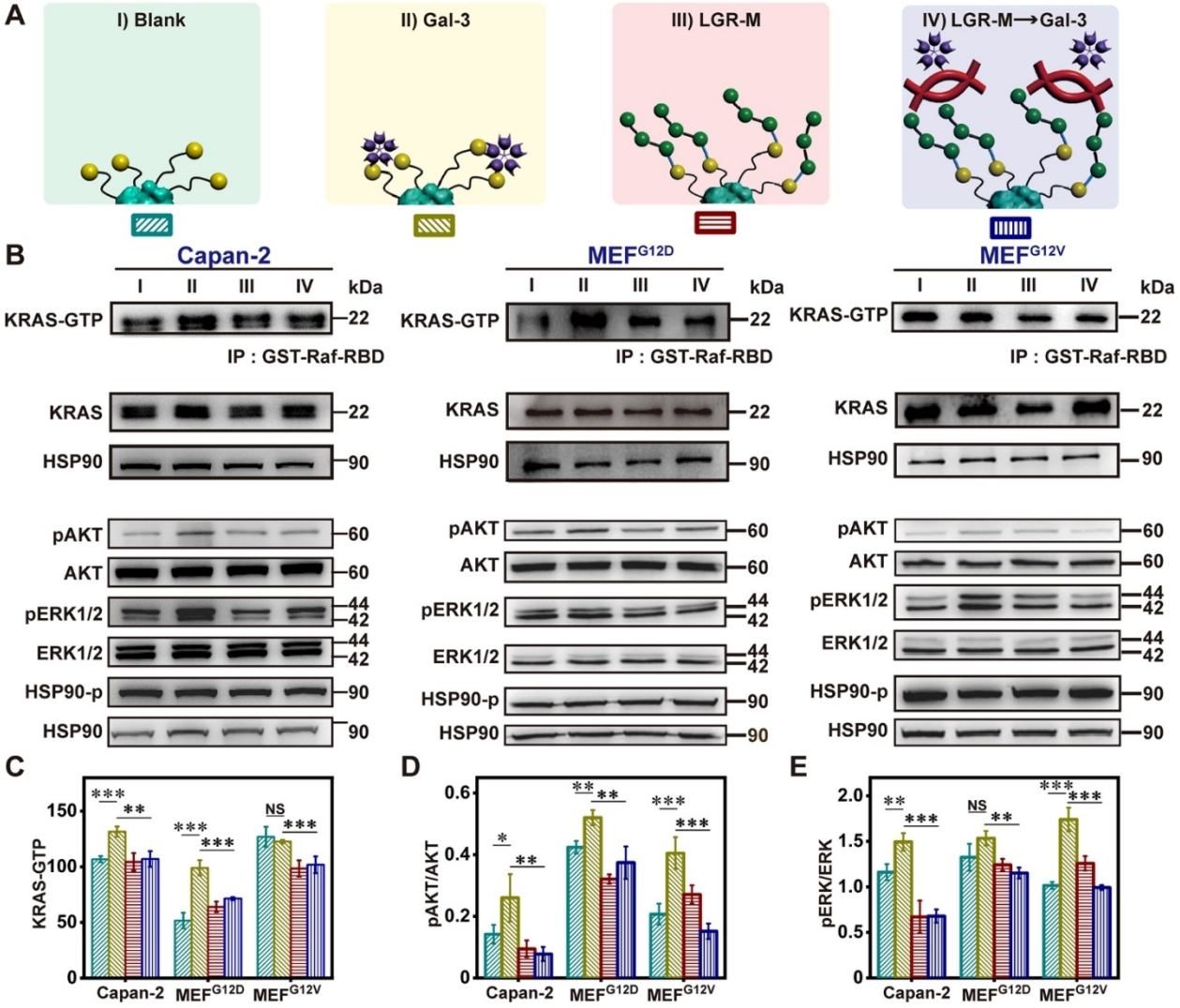

Figure 4. Blockade of $\alpha_v\beta_3$/Gal-3 interaction disrupts KRAS signaling. A) Scheme showing the four groups: Group I, untreated cells (blank); Group II, Gal-3 treated cells (Gal-3); Group III, LGR-M treated cells (LGR-M); Group IV, cells treated by LGR-M and then Gal-3 (LGR-M→Gal-3). B) The effect of different treatments on KRAS activation status in Capan-2 pancreatic cancer cells, and MEF cells with *KRAS*^{G12D} or *KRAS*^{G12V} mutations (MEF^{G12D}, MEF^{G12V}). C)–E) Quantification of the effect of different treatments on the levels of KRAS-GTP (C), pAKT/AKT (D), and pERK/ERK (E) in Capan-2, MEF^{G12D}, and MEF^{G12V} cells. The WB images shown are representative of three individual experiments, and the quantification results are shown as the mean ± SD, $n = 3$. * $p < 0.05$; ** $p < 0.005$; *** $p < 0.0005$; NS, not significant by one-way ANOVA.

and pERK levels (Figure 4B–E). Taken together, these results demonstrate the feasibility of intervening in KRAS signaling by performing glycan editing on upstream membrane receptor proteins.

Disruption of KRAS-Driven Malignant Phenotypes via Blocking $\alpha_v\beta_3$/Gal-3 Interaction

Finally, we investigated how Man_3 blockade of the $\alpha_v\beta_3$/Gal-3 interaction affects KRAS-driven malignant phenotypes, including oxidative stress detoxification and metastasis. It is well established that KRAS hyperactivation can protect cancer cells against oxidative stress and offer a survival advantage.[4] Thus, we monitored the intracellular reactive oxygen species (ROS) levels using a fluorescent ROS probe (2′,7′-dichlorofluorescin diacetate, DFCH) (Figure 5A).[34] As expected, all three $\alpha_v\beta_3$-positive cell lines in our study (Capan-2, A549, and MDA-MB-231) showed a sharp drop in intracellular ROS level after Gal-3 treatment for 1 h (Figure 5B), due to the activation of KRAS signaling[35] by Gal-3-mediated $\alpha_v\beta_3$ clustering. In contrast, when $\alpha_v\beta_3$ in these cells was modified by Man_3, the detoxification of ROS induced by Gal-3 was almost completely diminished (Figure 5A and B).

KRAS hyperactivation is also closely associated with a highly invasive phenotype through the activation of several nuclear transcription factors.[36] Thus, we performed both a cell scratch assay (Figure 5C and D) and a transwell migration assay (Figure 5E and F) to assess the influence of

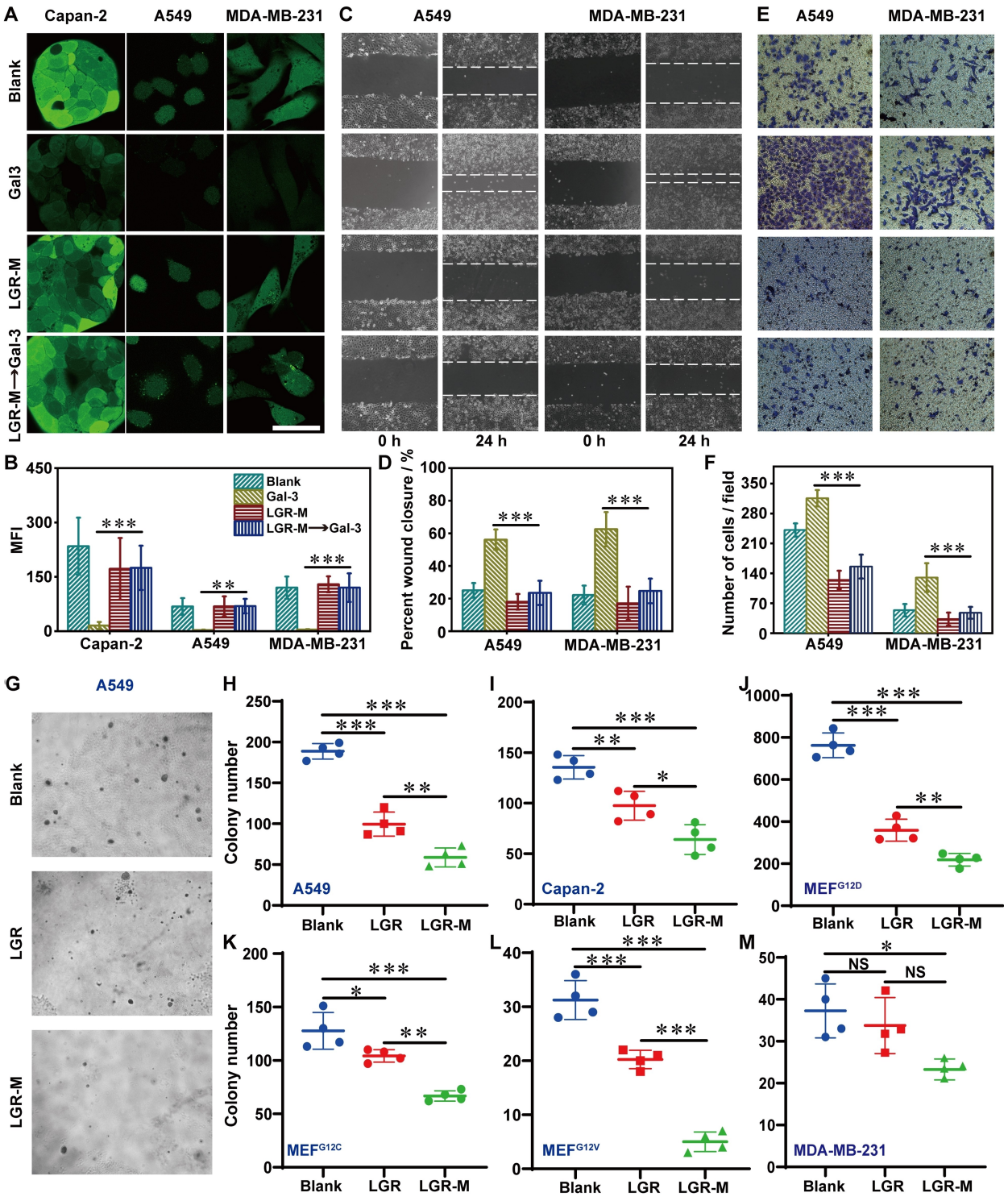

Figure 5. Effect of LGR-M on KRAS-driven phenotypes in cancer cells. A) ROS levels in Capan-2, A549, and MDA-MB-231 cells after different treatments were detected by DCFH staining. Scale bar: 50 μm. B) Quantification of the fluorescence signal from (A). C) Assessment of the horizontal migration capability of A549 and MDA-MB-231 cells after different treatments using a cell wound scratch assay. D) Quantification of cell migration rates from (C). The rate, represented by percent wound closure, was measured by dividing the migration area by the scratch area. E) Assessment of the vertical migration capability of A549 and MDA-MB-231 cells after different treatments using transwell migration assay. F) Quantification of migrated cells in (E). G)–M) 3D tumor spheroid formation assay after different treatments (blank, LGR, or LGR-M) using A549, Capan-2, MEFs, and MDA-MB-231 cell lines. G) Representative images of 3D tumor spheroid formation in A549 lung cancer cells. H)–M) Quantification of tumor spheroid formation for all six cell lines tested. Images in (A), (C), and (E) are representative of three individual experiments, and the quantification results in (B), (D), and (F) are shown as the mean ± SD, $n = 3$. The images in (G) are representative of two individual experiments with five replicates in each experiment, and the data shown in (H)–(M) are the mean ± SD, $n = 5$. Statistical differences in (B, D, F, H–M) were determined by one-way ANOVA. * $p < 0.05$; ** $p < 0.005$; *** $p < 0.0005$; NS, not significant.

LGR-M on the migration of A549 and MDA-MB-231 cells (the Capan-2 cell line displayed negligible migration, as manifested in Figure S25) in the presence of Gal-3. As shown in Figure 5C–F, LGR-M treatment significantly impaired the migration of A549 and MDA-MB-231 cells compared with the Gal-3 alone group. Furthermore, to mimic the real growth environment of tumors, we employed a 3D tumor spheroid formation assay on 6 cell lines (including 5 KRAS-mutant lines and 1 KRAS-wide type line (MDA-MB-231)) to evaluate the influence of LGR-M treatment on tumor proliferation (Figures 5G–M, S26). The 3D colony number in KRAS-mutant cell lines was significantly reduced in the LGR-M group compared with the LGR group even in the absence of exogenous Gal-3. Together, these effects of glycan editing on the malignant phenotypes of cancer cells are consistent with the inhibitory effect of LGR-M on Gal-3-elicited KRAS signaling, and strongly suggest glycan editing as a potential strategy to retard KRAS-driven cancers.

Conclusion

In this work, we designed a "localized oxidation-coupling" strategy for glycan editing, which has the following features: 1) Only the glycans on the POI are elongated with a chemically well-defined carbohydrate. This enables the direct observation and intervention of the biological effects of the glycoform of the POI. 2) This strategy does not have any restrictions on the structure of the donor sugars. 3) It is a multi-functional platform with built-in examination capability. Using the "localized oxidation-coupling" strategy, we successfully installed Man_3 on the glycan chains of $\alpha_v\beta_3$, which led to the blockade of $\alpha_v\beta_3$/Gal-3 interaction, the weakening of the activation of KRAS and downstream effectors, and the mitigation of KRAS-driven malignant phenotypes. These results provide solid evidence that $\alpha_v\beta_3$-specific blockade of Gal-3 binding is an indirect but efficient way to disrupt KRAS activation. Different from the global inhibition of Gal-3 binding using GCS-100 by the Cheresh group,[4] our method only blocks Gal-3 binding to $\alpha_v\beta_3$. The resultant protein specificity should lead to fewer side effects because Gal-3 also participates in other physiological processes,[37] whereas $\alpha_v\beta_3$ is mainly involved in cancer.[38] To our knowledge, this is the first successful attempt to interfere with KRAS activity by manipulating membrane receptor glycosylation.

In addition to $\alpha_v\beta_3$, other types of membrane receptors including EGFR and TGF-β also act as upstream activators of KRAS.[1,2] The proposed tool can be easily adapted to edit almost any cell surface glycoproteins by changing the recognition molecules (e.g. aptamers,[10,15,16] nanobodies[39]). The current glycan editing method is only applicable to cellular experiments. To adapt it for in vivo use, the key challenge is to achieve spatiotemporal control of GAO oxidation and Man_3 installation in vivo. Promising solutions include encapsulating c(RGDfK)-GAO and Man_3-H with targeted drug delivery & release systems or endowing GAO with controlled enzymatic activity. The installation of Man_3 at the in vivo level might facilitate the recognition of immune cells expressing mannose-binding lectins, thus acting as a regulator of the immune microenvironment.[40] In summary, our work provides a powerful tool to unveil and manipulate glycan functions in a protein-specific fashion, which holds great potential for the development of glycan-targeting therapeutic approaches, especially for "undruggable" KRAS-driven cancers.

Acknowledgements

We would like to thank Prof. Ran Xie (Nanjing University) for the helpful discussion. We also gratefully acknowledge support from the National Natural Science Foundation of China (21974067, 22274073, 21877060, 21890741, 21708019), Fundamental Research Funds for the Central Universities (020514380309, 021414380502, 2022300324, 021114380173), and the State Key Laboratory of Analytical Chemistry for Life Science (5431ZZXM2204).

Conflict of Interest

The authors declare no conflict of interest.

Data Availability Statement

The data that support the findings of this study are available from the corresponding author upon reasonable request.

Keywords: Galactose Oxidase · Glycan Editing · Glycoproteins · KRAS · Protein-Specific

[1] A. D. Cox, S. W. Fesik, A. C. Kimmelman, J. Luo, C. J. Der, *Nat. Rev. Drug Discovery* **2014**, *13*, 828–851.
[2] A. R. Moore, S. C. Rosenberg, F. McCormick, S. Malek, *Nat. Rev. Drug Discovery* **2020**, *19*, 533–552.
[3] L. Seguin, S. Kato, A. Franovic, M. F. Camargo, J. Lesperance, K. C. Elliott, M. Yebra, A. Mielgo, A. M. Lowy, H. Husain, T. Cascone, L. Diao, J. Wang, I. I. Wistuba, J. V. Heymach, S. M. Lippman, J. S. Desgrosellier, S. Anand, S. M. Weis, D. A. Cheresh, *Nat. Cell Biol.* **2014**, *16*, 457–468.
[4] L. Seguin, M. F. Camargo, H. I. Wettersten, S. Kato, J. S. Desgrosellier, T. von Schalscha, K. C. Elliott, E. Cosset, J. Lesperance, S. M. Weis, D. A. Cheresh, *Cancer Discovery* **2017**, *7*, 1464–1479.
[5] J. Canon, K. Rex, A. Y. Saiki, C. Mohr, K. Cooke, D. Bagal, K. Gaida, T. Holt, C. G. Knutson, N. Koppada, B. A. Lanman, J. Werner, A. S. Rapaport, T. S. Miguel, R. Ortiz, T. Osgood, J.-R. Sun, X. Zhu, J. D. McCarter, L. P. Volak, B. E. Houk, M. G. Fakih, B. H. O'Neil, T. J. Price, G. S. Falchook, J. Desai, J. Kuo, R. Govindan, D. S. Hong, W. Ouyang, H. Henary, T. Arvedson, V. J. Cee, J. R. Lipford, *Nature* **2019**, *575*, 217–223.
[6] S. Kamerkar, V. S. LeBleu, H. Sugimoto, S. Yang, C. F. Ruivo, S. A. Melo, J. J. Lee, R. Kalluri, *Nature* **2017**, *546*, 498–503.
[7] E. S. Leshchiner, A. Parkhitko, G. H. Bird, J. Luccarelli, J. A. Bellairs, S. Escudero, K. Opoku-Nsiah, M. Godes, N. Perrimon, L. D. Walensky, *Proc. Natl. Acad. Sci. USA* **2015**, *112*, 1761–1766.

[8] K. T. Schjoldager, Y. Narimatsu, H. J. Joshi, H. Clausen, *Nat. Rev. Mol. Cell Biol.* **2020**, *21*, 729–749.
[9] Y. Zeng, T. N. C. Ramya, A. Dirksen, P. E. Dawson, J. C. Paulson, *Nat. Methods* **2009**, *6*, 207–209.
[10] P. V. Robinson, G. de Almeida-Escobedo, A. E. de Groot, J. L. McKechnie, C. R. Bertozzi, *J. Am. Chem. Soc.* **2015**, *137*, 10452–10455.
[11] J. Li, M. Chen, Z. Liu, L. Zhang, B. H. Felding, K. W. Moremen, G. Lauvau, M. Abadier, K. Ley, P. A. Wu, *ACS Cent. Sci.* **2018**, *4*, 1633–1641.
[12] F. Tang, M. Zhou, K. Qin, W. Shi, A. Yashinov, Y. Yang, L. Yang, D. Guan, L. Zhao, Y. Tang, Y. Chang, L. Zhao, H. Yang, H. Zhou, R. Huang, W. Huang, *Nat. Chem. Biol.* **2020**, *16*, 766–775.
[13] Y. Ge, D. H. Ramirez, B. Yang, A. K. D'Souza, C. Aonbangkhen, S. Wong, C. M. Woo, *Nat. Chem. Biol.* **2021**, *17*, 593–600.
[14] H. Xiao, E. C. Woods, P. Vukojicic, C. R. Bertozzi, *Proc. Natl. Acad. Sci. USA* **2016**, *113*, 10304–10309.
[15] J. Hui, L. Bao, S. Li, Y. Zhang, Y. Feng, L. Ding, H. Ju, *Angew. Chem. Int. Ed.* **2017**, *56*, 8139–8143.
[16] Y. Guo, J. Tao, Y. Li, Y. Feng, H. Ju, Z. Wang, L. Ding, *J. Am. Chem. Soc.* **2020**, *142*, 7404–7412.
[17] J.-Y. Byeon, F. T. Limpoco, R. C. Bailey, *Langmuir* **2010**, *26*, 15430–15435.
[18] M. Pfaff, K. Tangemann, B. Müller, M. Gurrath, G. Müller, H. Kessler, R. Timpl, J. Engel, *J. Biol. Chem.* **1994**, *269*, 20233–20238.
[19] J. B. Rannes, A. Ioannou, S. C. Willies, G. Grogan, C. Behrens, S. L. Flitsch, N. J. Turner, *J. Am. Chem. Soc.* **2011**, *133*, 8436–8439.
[20] E. Pocheć, M. Bubka, M. Rydlewska, M. Janik, M. Pokrywka, A. Lityńska, *Anticancer Res.* **2015**, *35*, 2093–2103.
[21] G. Marsico, L. Russo, F. Quondamatteo, A. Pandit, *Trends Cancer* **2018**, *4*, 537–552.
[22] J. Shen, L. Jia, L. Dang, Y. Su, J. Zhang, Y. Xu, B. Zhu, Z. Chen, J. Wu, R. Lan, Z. Hao, C. Ma, T. Zhao, N. Gao, J. Bai, Y. Zhi, J. Li, J. Zhang, S. Sun, *Nat. Methods* **2021**, *18*, 921–929.
[23] N. Tamilarasu, J. Zhang, S. Hwang, T. M. Rana, *Bioconjugate Chem.* **2001**, *12*, 135–138.
[24] A. Heifetz, R. W. Keenan, A. D. Elbein, *Biochemistry* **1979**, *18*, 2186–2192.
[25] F. Ulloa, F. X. Real, *J. Biol. Chem.* **2003**, *278*, 12374–12383.
[26] R. L. Whistler, C. G. Smith, *J. Am. Chem. Soc.* **1952**, *74*, 3795–3796.
[27] P. S. Gonzalez, J. O'Prey, S. Cardaci, V. J. A. Barthet, J.-I. Sakamaki, F. Beaumatin, A. Roseweir, D. M. Gay, G. Mackay, G. Malviya, E. Kania, S. Ritchie, A. D. Baudot, B. Zunino, A. Mrowinska, C. Nixon, D. Ennis, A. Hoyle, D. Millan, I. A. McNeish, O. J. Sansom, J. Edwards, K. M. Ryan, *Nature* **2018**, *563*, 719–723.
[28] Y. Zhang, J.-H. Zhao, X.-Y. Zhang, H.-B. Guo, F. Liu, H.-L. Chen, *Mol. Cell. Biochem.* **2004**, *260*, 137–146.
[29] N. S. Flinn, M. Quibell, T. P. Monk, M. K. Ramjee, C. J. Urch, *Bioconjugate Chem.* **2005**, *16*, 722–728.
[30] H. Lis, N. Sharon, *Chem. Rev.* **1998**, *98*, 637–674.
[31] N. C. Henderson, A. C. Mackinnon, S. L. Farnworth, F. Poirier, F. P. Russo, J. P. Iredale, C. Haslett, K. J. Simpson, T. Sethi, *Proc. Natl. Acad. Sci. USA* **2006**, *103*, 5060–5065.
[32] J. Dumic, S. Dabelic, M. Flögel, *Biochim. Biophys. Acta Gen. Subj.* **2006**, *1760*, 616–635.
[33] S. Song, B. Ji, V. Ramachandran, H. Wang, M. Hafley, C. Logsdon, R. S. Bresalier, *PLoS One* **2012**, *7*, e42699.
[34] R. Wang, M. Shi, F. Xu, Y. Qiu, P. Zhang, K. Shen, Q. Zhao, J. Yu, Y. Zhang, *Nat. Commun.* **2020**, *11*, 4465.
[35] G. M. DeNicola, F. A. Karreth, T. J. Humpton, A. Gopinathan, C. Wei, K. Frese, D. Mangal, K. H. Yu, C. J. Yeo, E. S. Calhoun, F. Scrimieri, J. M. Winter, R. H. Hruban, C. Iacobuzio-Donahue, S. E. Kern, I. A. Blair, D. A. Tuveson, *Nature* **2011**, *475*, 106–109.
[36] L. Buscail, B. Bournet, P. Cordelier, *Nat. Rev. Gastroenterol. Hepatol.* **2020**, *17*, 153–168.
[37] R. Dong, M. Zhang, Q. Hu, S. Zheng, A. Soh, Y. Zheng, H. Yuan, *Int. J. Mol. Med.* **2018**, *41*, 599–614.
[38] H. Hamidi, J. Ivaska, *Nat. Rev. Cancer* **2018**, *18*, 533–548.
[39] N. Pishesha, T. Harmand, L. Y. Smeding, W. Ma, L. S. Ludwig, R. Janssen, A. Islam, Y. J. Xie, T. Fang, N. McCaul, W. Pinney III, H. R. Sugito, M. A. Rossotti, G. Gonzalez-Sapienza, H. L. Ploegh, *Nat. Biomed. Eng.* **2021**, *5*, 1389–1401.
[40] J. M. Jaynes, R. Sable, M. Ronzetti, W. Bautista, Z. Knotts, A. Abisoye-Ogunniyan, D. Li, R. Calvo, M. Dashnyam, A. Singh, T. Guerin, J. White, S. Ravichandran, P. Kumar, K. Talsania, V. Chen, A. Ghebremedhin, B. Karanam, A. B. Salam, R. Amin, T. Odzorig, T. Aiken, V. Nguyen, Y. Bian, J. C. Zarif, A. E. de Groot, M. Mehta, L. Fan, X. Hu, A. Simeonov, N. Pate, M. Abu-Asab, M. Ferrer, N. Southall, C.-Y. Ock, Y. Zhao, H. Lopez, S. Kozlov, N. de Val, C. C. Yates, B. Baljinnyam, J. Marugan, U. Rudloff, *Sci. Transl. Med.* **2020**, *12*, eaax6337.

Manuscript received: December 8, 2022
Accepted manuscript online: April 27, 2023
Version of record online: ■■, ■■

Research Articles

Glycan Editing

Y. Li, F. Huo, L. Chen, H. Wang, J. Wu, P. Zhang, N. Feng, W. Li, L. Wang, Y. Wang, X. Wang, X. Yang, Z. Lu, Y. Mao, C. Yan,* L. Ding,* H. Ju

Protein-Targeted Glycan Editing on Living Cells Disrupts KRAS Signaling

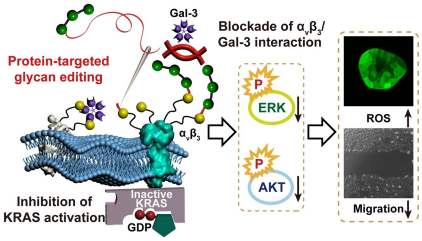

A protein-targeted glycan editing strategy is developed for interfering with KRAS activity by manipulating the glycosylation of upstream membrane receptors. The attachment of mannotriose to the terminal galactose/*N*-acetyl-D-galactosamine epitopes of integrin $\alpha_v\beta_3$ blocks its binding with galectin-3, suppresses the activation of KRAS and downstream effectors, and mitigates KRAS-driven malignant phenotypes.